[CANCER RESEARCH 64, 6002–6009, September 1, 2004]

Identification of Aberrantly Methylated Genes in Association with Adult T-Cell Leukemia

Jun-ichirou Yasunaga,[1] Yuko Taniguchi,[1] Kisato Nosaka,[1] Mika Yoshida,[1] Yorifumi Satou,[1] Tatsunori Sakai,[2] Hiroaki Mitsuya,[2] and Masao Matsuoka[1]

[1]Laboratory of Virus Immunology, Institute for Virus Research, Kyoto University, Kyoto, Japan; and [2]Department of Internal Medicine II, Kumamoto University School of Medicine, Kumamoto, Japan

ABSTRACT

In this study, we identified 53 aberrantly hypermethylated DNA sequences in adult T-cell leukemia (ATL) cells using methylated CpG island amplification/representational difference analysis method. We also observed a proportionate increase in the methylation density of these regions with disease progression. Seven genes, which were expressed in normal T cells, but suppressed in ATL cells, were identified near the hypermethylated regions. Among these silenced genes, *Kruppel-like factor 4* (*KLF4*) gene is a cell cycle regulator and *early growth response 3* (*EGR3*) gene is a critical transcriptional factor for induction of Fas ligand (FasL) expression. Treatment with 5-aza-2′-deoxycytidine resulted in the recovery of their transcription, indicating that their silencing might be associated with DNA hypermethylation. To study their functions in ATL cells, we transfected recombinant adenovirus vectors expressing *KLF4* and *EGR3* genes. Expression of *KLF4* induced apoptosis of ATL cells whereas enforced expression of *EGR3* induced the expression of *FasL* gene, resulting in apoptosis. Thus, suppressed expression of *EGR3* enabled ATL cells to escape from activation-induced cell death mediated by FasL. Our results showed that the methylated CpG island amplification/representational difference analysis method allowed the isolation of hypermethylated DNA regions specific to leukemic cells and thus shed light on the roles of DNA methylation in leukemogenesis.

INTRODUCTION

Human T-cell leukemia virus type I (HTLV-I) is the causative retrovirus of a neoplastic disease, adult T-cell leukemia (ATL) and an inflammatory disease, HTLV-I-associated myelopathy/tropical spastic paraparesis (1–4). After infection with HTLV-I, a small proportion of carriers (about 2–5%) develop ATL after a long latent period (5). In this virus-induced leukemia, viral proteins encoded by HTLV-I play an important role in the proliferation of infected cells and leukemogenesis. Among them, Tax is considered to play a central role in leukemogenesis because of its pleiotropic actions (6, 7), such as transcriptional activation of cellular genes (8–10), *trans*-repression of cellular genes transcription (11, 12), and functional inactivation of p53 and MAD1 (12, 13). These pleiotropic functions render HTLV-I-infected cells able to proliferate, and confer resistance to apoptotic signals, resulting in clonal expansion.

In the late stage of leukemogenesis, *tax* is frequently inactivated through several mechanisms (14) such as loss of 5′-long terminal repeat (LTR) (15), genetic alterations of *tax* gene (16), and DNA hypermethylation in 5′-LTR (17), indicating that Tax is not always necessary for leukemogenesis. Because Tax is the major target molecule of CTLs *in vivo* (18), the expression of Tax confers a growth advantage to infected cells, but on the other hand, it renders infected cells susceptible to CTLs. Fully transformed ATL cells are considered to acquire the ability to proliferate *in vivo* in the absence of Tax expression. Such a transformation process is thought to include alterations of host genome: genetic and epigenetic changes. Although the genetic changes, such as mutation of *p53* (19) and deletion of *p16* (20, 21), in ATL cells were reported, they are not frequent and are observed predominantly in the late stage of the disease.

In addition to genetic alterations, DNA hypermethylation of promoter region CpG islands has been analyzed in the context of oncogenesis because this process silences gene transcription of tumor-suppressor genes. This epigenetic alteration is observed commonly in various cancer cells. Although methylation "profiling" studies have shown that some genes are frequently methylated in various tumor cells, other genes are methylated in a tumor-type-specific manner (22, 23). To date, several methods have been developed to isolate differentially methylated DNA regions in cancers (24–29). Recently, with methylated CpG island amplification/representational difference analysis (MCA/RDA) method, we isolated hypomethylated DNA regions and demonstrated that *MEL1S* gene was hypomethylated and aberrantly transcribed in ATL cells (30).

The present study was designed to isolate hypermethylated DNA regions in ATL cells compared with cells in the carrier state using the MCA/RDA method and to identify those genes that have an expression associated with DNA hypermethylation. On the basis of our results, we discuss the association between aberrant DNA methylation and leukemogenesis of ATL.

MATERIALS AND METHODS

Cells. Peripheral blood mononuclear cells (PBMCs) were isolated from 10 patients with ATL (five acute type cases and five chronic type cases), five asymptomatic carriers, and five uninfected individuals using Ficoll-Paque density centrifugation method. We also used the cell lines ED, ATL-43T, ATL-48T, ATL-55T, MT-1, and TL-Om1, which were derived from leukemic clones, and MT-2, which is derived from nonleukemic cells. To study the effect of demethylation, ATL-43T was cultured in media supplemented with 10 μmol/l 5-aza-2′-deoxycytidine (5-aza-dC; Sigma, St. Louis, MO) for 3 days, 10 μmol/l 5-aza-dC and 1 μmol/l trichostatin A (TSA; Sigma) for the last 24 hours, or 1 μmol/l TSA for 24 hours alone. The human embryonic kidney cell line, HEK 293, was used for the packaging of recombinant adenovirus vectors.

Viral FLICE-inhibitory protein (FLIP) derived from the equine herpes virus type 2, E8 (31), and the long form of murine cellular FLIP ($mCasper_L$; Ref. 32) expression vectors were transfected into ATL-43T cells by electroporation with a Gene Pulser II (Bio-Rad, Hercules, CA). Stable transfectants were selected and maintained in culture medium containing G418 (500 μg/ml; Nacalai tesque, Kyoto, Japan). The transfected cell lines by each of the vectors were designated as ATL-43T-E8 and ATL-43T-mCas, respectively.

Methylated CpG Island Amplification/Representational Difference Analysis. To identify aberrantly hypermethylated DNA regions in ATL cells, we used the MCA/RDA method, as reported previously (28). Five micrograms of genomic DNA were digested with 100 units of *Sma*I (New England Biolabs, Beverly, MA) twice and then digested once with 20 units of *Xma*I (New England Biolabs). RMCA adaptor was prepared by annealing of the oligonucleotides RMCA24 (5′-CCACCGCCATCCGAGCCTTTCTGC-3′) and

Received 4/26/04; revised 6/15/04; accepted 6/25/04.

Grant support: Grant-in-Aid for Scientific Research from the Ministry of Education, Science, Sports, and Culture of Japan.

The costs of publication of this article were defrayed in part by the payment of page charges. This article must therefore be hereby marked *advertisement* in accordance with 18 U.S.C. Section 1734 solely to indicate this fact.

Note: Supplementary data for this article can be found at Cancer Research Online (http://cancerres.aacrjournals.org).

Requests for reprints: Jun-ichirou Yasunaga, Laboratory of Virus Immunology, Institute of Virus Research, Kyoto University, Kyoto 606-8507, Japan. Phone: 81-75-751-4048; Fax: 81-75-751-4049; E-mail: jyasunag@virus.kyoto-u.ac.jp.

RMCA12 (5′-CCGGGCAGAAAG-3′), and ligated to the digested DNA fragments using T4 DNA ligase (New England Biolabs). To amplify the hypermethylated DNA fragments, which were ligated adaptors in both ends, PCR was performed using the RMCA24 oligonucleotides as primers. The amplicons were synthesized using samples from an ATL patient and a HTLV-I carrier. For detection of ATL cell-specific hypermethylated DNA sequences, MCA products from a carrier were used as a driver of RDA, and those products from an acute ATL patient as a tester. We used GeneFisher Basic Reagent Set (TaKaRa, Shiga, Japan) for RDA. In RDA step, 500 and 100 ng of ligation mixture were used for the first and second selective PCR, respectively. Oligonucleotides used for RDA were JMCA24 (5′-GTGAGGGTCGGATCTGGATGGCTC-3′), JMCA12 (5′CCGGGAGCCAGC-3′), NMCA24 (5′-GTTAGCGGACACAGGGCGGGTCAC-3′), and NMCA12 (5′-CCGGGTGACCCG-3′). Subcloning of the MCA/RDA products was carried out using pCR-XL-TOPO (Invitrogen, Carlsbad, CA) or pGEM-T Easy (Promega, Madison, WI) as vectors, and then the sequences of each fragment were determined by PCR using M13 primers. Sequence homologies and localization in chromosomes were identified using the BLAST program of the National Center for Biotechnology Information.[3]

MCA-Southern Hybridization. To confirm that the isolated DNA regions are specifically hypermethylated in ATL cells, Southern blot method was used. MCA products from an ATL patient and a HTLV-I carrier (500-ng each) were separated by electrophoresis in 1.5% agarose gels and then transferred to Hybond-N + (Amersham Biosciences, Piscataway, NJ). All of the isolated DNA fragments were labeled with ^{32}P, and hybridized to these filters.

Combined Bisulfite Restriction Analysis and Bisulfite Sequencing Analysis. For nine DNA regions identified by MCA/RDA, the methylation status of the DNA regions was determined by Combined Bisulfite Restriction Analysis or bisulfite sequencing as described previously (33). First, genomic DNAs were treated with sodium bisulfite (34) and then amplified by nested PCR using the specific primers listed in Supplementary Table 1. The PCR products of these regions were digested with *Taq*I (New England Biolabs) or *Acc*II (TaKaRa), subjected to electrophoresis in 3% agarose gels, and visualized by ethidium bromide staining. The percentage of DNA methylation was calculated by the intensities of methylation and unmethylation signal determined by ATTO densitometry software (ATTO, Tokyo, Japan).

For detailed analysis of DNA methylation in *Kruppel-like factor 4* (*KLF4*) and *early growth response 3* (*EGR3*) genes, we performed bisulfite sequencing. The PCR products of the isolated regions and promoter regions of these genes were subcloned into pGEM-T Easy, thereafter, the sequences of each of 10 clones were determined. Because the promoter sequence of *KLF4* has not been determined, we predicted its sequence using the program[4] supported by the BioInformatics & Molecular Analysis Section, Computational Bioscience and Engineering Lab, Center for Information Technology, and NIH. Primers for bisulfite sequencing are also listed in Supplementary Table 1.

Semi-quantitative Reverse Transcriptase-PCR. Total RNA was extracted from the PBMCs and cell lines using Trizol reagent (Invitrogen) and then treated DNaseI (Invitrogen). cDNAs were synthesized from 0.5 μg of total RNA with the Superscript First-Strand Synthesis System for reverse transcription (RT)-PCR (Invitrogen) and used for semi-quantitative RT-PCR as template. The primers used for RT-PCR and their annealing temperatures are summarized in Supplementary Table 2. The number of PCR cycles was appropriately determined for each quantification (Supplementary Table 2). We used 1.25 units of ExTaq polymerase (TaKaRa) for each reaction. All experiments were performed including samples of whole brain (Clontech, Palo Alto, CA) and skeletal muscle (Stratagene, La Jolla, CA) as positive control of PCR reaction.

Construction of Adenovirus Vectors. The recombinant adenovirus vectors containing *KLF4* and *EGR3* gene (KLF4-AD and EGR3-AD, respectively) were generated using Adeno-X Expression System (Clontech) according to the manufacturer's protocol. These adenovirus vectors were concentrated and purified by Virakit for adenovirus 5 and recombinant derivatives (Virapur, San Diego, CA), and then the viral titers were determined using Adeno-X Rapid Titer Kit (Clontech). The *lacZ*-containing adenovirus vector (lacZ-AD) was also prepared as a negative control. All adenovirus vectors were used to infect an ATL cell line, ATL-43T, at 1,000 infectious units/cell.

Flow Cytometric Analysis. The flow cytometry (model EPICS XL flow cytometer, Beckman Coulter, Miami Lakes, FL) was used for analyses of apoptosis. Annexin V-FITC/PI double staining and terminal-deoxynucleotidyl transferase-mediated dUTP-FITC nick-end labeling (TUNEL) assay were performed for detection of apoptosis, using MEBCYTO apoptosis kit (MBL, Nagoya, Japan) and MEBSTEIN apoptosis kit direct (MBL), respectively.

RESULTS

Isolation of Hypermethylated DNA Regions in the Genome from ATL Cells. To identify hypermethylated regions in the genome of ATL cells, we carried out MCA/RDA, which was used previously to isolate a number of methylated CpG islands in colon cancer cell line (28). MCA products were generated from the genomic DNA of a carrier (driver) and an acute ATL patient (tester). After the second round of RDA, the PCR products were subcloned, and their sequences were determined. To confirm that identified DNA fragments were amplified in tester amplicon, we examined whether isolated DNA fragment specifically hybridized to the tester amplicon using Southern blot method (MCA-Southern). Specific hybridization to the tester amplicon implied that isolated DNA regions were hypermethylated in ATL cells compared with peripheral blood mononuclear cell (PBMC) from a carrier. Finally, we identified 53 differentially hypermethylated DNA fragments in ATL cells. The chromosomal locations of all of the fragments were analyzed by NCBI BLAST program. We tested whether these identified regions satisfied the criteria for CpG islands proposed by Takai and Jones (35). The results revealed that the majority of clones (48 of 53 clones) were located in CpG islands. Information of isolated sequences is described in Table 1.

Accumulation of Aberrant DNA Hypermethylation during Disease Progression. Chronic ATL is characterized as an indolent form, which later progresses to aggressive forms (*i.e.*, acute or lymphoma-type ATL). To confirm that DNA hypermethylation identified in this study is associated with disease progression, we analyzed the extent of DNA methylation of nine DNA regions at different stages by Combined Bisulfite Restriction Analysis. Fig. 1*A* shows the profiles of the methylation status in these DNA fragments. In cell lines, CpG sites in identified DNA fragments were highly methylated, which was consistent with the finding of DNA methylation in the established cell lines. This confirmed that the isolated DNA regions were hypermethylated in ATL cells and that MCA-Southern could identify the hypermethylated DNA regions. In the carrier state, most DNA fragments were unmethylated. On the other hand, they were frequently methylated in chronic ATL, and the level of methylation increased in acute ATL, indicating that DNA methylation in the isolated DNA regions tends to accumulate according to disease progression. This was also confirmed in the sequential samples from a HTLV-I carrier, who developed acute ATL (Fig. 1*B*).

Identification of Genes near the Hypermethylated DNA Regions. To analyze the influence of identified DNA hypermethylation upon gene transcription, the neighboring genes were searched using NCBI BLAST program as described in Materials and Methods. We found that 31 of 53 (58%) clones were located within the exon or intron of the gene, and 41 of 53 (77%) loci were located within 10 kb from the transcriptional start site of the nearest gene (Table 1). Because the aberrant methylation of some identified genes, such as *PAX5* (clone 10; ref. 36) and *CSPG2* (clone 27; ref. 28), have been reported in various types of cancer cells, it confirmed that MCA/RDA method in this study isolated the hypermethylated DNA regions. Then, we analyzed the transcription of genes in which the transcriptional start sites existed within 2 kb from the identified hypermethylated DNA regions (Fig. 2). On the basis of their expression profiles, we could divide the genes identified into two groups; group I con-

[3] http://www.ncbi.nlm.nih.gov/BLAST/.
[4] http://bimas.dcrt.nih.gov:80/molbio/proscan/.

Table 1 *Characterization of DNA fragments isolated by MCA/RDA*

Clone	Size (bp)	Accession no. (location)	Chromosomal location	Nearest gene	CpG Island	Distance from TSS (bp)
1	733	NT_007592.13 (19499884–19500616)	6p21.31	*No gene**	Yes	
2	511	NT_006713.13 (6324465–6324975)	5q13.3	*OTP*	Yes	2,600
3	377	NT_025741.13 (5075242–5075619)	6q16.3	*SIM1*	Yes	5,800
4	486	NT_079617.1 (40630–41115)	4p16.1	*HMX1*	Yes	200
5	577	NT_016354.16 (9912331–9912907)	4q21.3	*NKX6–1*	Yes	700
6	418	NT_009237.16 (13859103–13859520)	11p15.2	*CALCB*	Yes	50
7	673	NT_011109.15 (19265899–19266571)	19q13.33	*No gene*	Yes	
8	746	NT_022184.13 (23995750–23996496)	2p21	*LOC375201*	Yes	7,600
9	923	NT_026437.10 (32654509–32655429)	14q22.1	*PTGDR*	Yes	40
10	894	NT_008413.16 (37015465–37016356)	9p13	*PAX5*	Yes	8,100
11	533	NT_030059.11 (38044642–38045174)	10q26.1	*EMX2*	Yes	5,300
12	651	NT_010505.14 (1424933–1425583)	16q12.1	*CBLN1*	Yes	680
13	568	NT_007592.13 (1276022–1276589)	6p24	*TFAP2A*	Yes	2,500
14	725	NT_008583.16 (25707371–25708095)	10q22.3	*MGC2555*	Yes	4,500
15	591	NT_079592.1 (49215607–49216197)	7p12.1	*LOC378069*	Yes	190
16	424	NT_023666.16 (1934093–1934516)	8p21.2	*No gene*	Yes	
17	806	NT_009237.16 (30583999–30584804)	11p13	*No gene*	Yes	
18	696	NT_016354.16 (58568060–58568755)	4q28.3	*PCDH10*	Yes	2,500
19	620	NT_079596.1 (7038723–7039342)	7q22	*LAMB1*	Yes	720
20	937	NT_007592.13 (17472263–17473201)	6p21.1	*No gene*	Yes	
21	462	NT_008183.17 (7857852–7858312)	8q11.23	*KIAA1889*	Yes	290
22	487	NT_008470.16 (11911721–11912207)	9q31	*KLF4*	Yes	1,100
23	893	NT_025741.13 (12657384–12658276)	6q21	*NR2E1*	Yes	690
24	750	NT_079592.1 (23721242–23721991)	7p15.1	*NPY*	Yes	370
25	766	NT_077451.3 (1864762–1865527)	5qter	*ADAMTS2*	Yes	1,800
26	607	NT_004610.16 (1272547–1273153)	1p35	*PLA2G2F*	No	2,600
27	404	NT_006713.13 (12160670–12161073)	5q14.3	*CSPG2*	Yes	960
28	521	NT_023666.16 (922959–923479)	8p21.2	*EGR3*	Yes	1,700
29	895	NT_029419.10 (19759986–19760882)	12q13.2	*NXPH4*	No	6,100
30	430	NT_079593.1 (2760886–2761315)	7q11	*No gene*	No	
31	476	NT_011362.8 (4369966–4370441)	20q12	*MAFB*	Yes	350
32	878	NT_033903.6 (11275620–11276497)	11q13.1	*RIN1*	No	550
33	732	NT_009755.16 (3985255–3985983)	12q24.32	*No gene*	Yes	
34	795	NT_026437.10 (16902942–16903736)	14q13	*LOC253970*	Yes	340
35	530	NT_004671.15 (9240059–9240588)	1q31	*LHX9*	Yes	920
36	724	NT_005334.14 (10987626–10988353)	2p24.1	*No gene*	Yes	
37	943	NT_009237.16 (31223373–31224306)	11p13	*WIT-1*	Yes	40
38	587	NT_077921.1 (573714–574300)	1p36.13	*PAX7*	Yes	660
39	273	BX649589.3 (5548–5821)	9q34.3	*AGS3*	Yes	6,100
40	755	NT_022184.13 (8050474–8051228)	2p23.3	*No gene*	No	
41	958	NT_010783.14 (18185717–18186674)	17q22	*TBX4*	Yes	200
42	871	NT_005403.14 (27236075–27236942)	2q31.1	*HOXD3*	Yes	1,300
43	470	NT_030059.11 (21731229–21731698)	10q24	*LBX1*	Yes	5,500
44	406	NT_008818.15 (769699–770104)	10q26.2	*LOC338623*	Yes	230
45	565	NT_023935.16 (8798224–8798788)	9q21	*No gene*	Yes	
46	526	NT_010194.16 (47422212–47422737)	15q23	*ISL2*	Yes	2,700
47	445	NT_029289.10 (9369340–9369784)	5q32	*ADRB2*	Yes	230
48	414	NT_023133.11 (17468804–17469217)	5q34	*NKX2–5*	Yes	2,600
49	583	NT_022792.16 (6841497–6842079)	4q33	*No gene*	Yes	
50	1096	NT_026437.10 (18598721–18599816)	14q13	*SSTR1*	Yes	1,500
51	608	NT_077812.2 (1002922–1003529)	19p13.3	*FLJ46061*	Yes	8,600
52	310	NT_006713.13 (1986840–1987149)	5q13.3	*No gene*	Yes	
53	465	NT_011512.9 (8031349–8031813)	21q21.1	*NCAM2*	Yes	690

Abbreviation: TSS, transcription start site.
* "*No gene*" means TSS of the nearest gene is more than 10 kb away from the isolated region.

tained genes with an expression that was observed in activated T lymphocytes but suppressed in HTLV-I-transformed and ATL cell lines (Fig. 2*A*). On the other hand, the transcription of genes in group II was not detected in activated T cells and HTLV-I-associated cell lines whereas their expression was found in the brain and/or skeletal muscle (Fig. 2*B*). Group II genes were hypermethylated only in ATL cells but not in normal T lymphocytes. These results suggest that the suppressed expression of group I genes is implicated in leukemogenesis.

Relationship between Silencing of Neighboring Genes and DNA Methylation. We studied the detailed DNA methylation status in the promoter and isolated regions of *KLF4* and *EGR3* genes, which belong to group I, using the bisulfite sequencing method. The sequences of each of the 10 clones are summarized in Fig. 3. In both ATL-43T and an acute ATL, the CpGs in the isolated region of *KLF4* gene, which existed in exon 3, were heavily methylated (Fig. 3*A*) whereas there was little methylation in normal PBMCs. In the predicted *KLF4* promoter sequence, there was dense DNA methylation in ATL-43T and mild methylation in fresh ATL cells whereas the CpGs in normal PBMC were little methylated (Fig. 3*A*). DNA methylation in the promoter region of *KLF4* has been studied in primary cells with different stage of ATL to analyze the association with disease progression (Fig. 3*B*). DNA methylation increased according to disease progression from carrier to leukemia although there was little difference between chronic and acute ATL. In the case of the *EGR3* gene, the isolated region, which was in exon 2, was hypermethylated in the ATL cell line and fresh ATL cells but hypomethylated in normal PBMC (Fig. 3*C*). Although the promoter region of *EGR3* was hypermethylated in the ATL cell line, it was not methylated in fresh ATL cells and normal PBMCs.

Next, we analyzed whether the transcriptions of these silenced genes could be recovered by the demethylating agent, 5-aza-dC, and/or a histone deacetylase inhibitor, TSA in ATL cells. The combination of 5-aza-dC and TSA is known to induce a synergistic effect on DNA demethylation (37). As shown in Fig. 2*C*, the transcripts of *KLF4* gene were re-expressed by 5-aza-dC alone or by combination

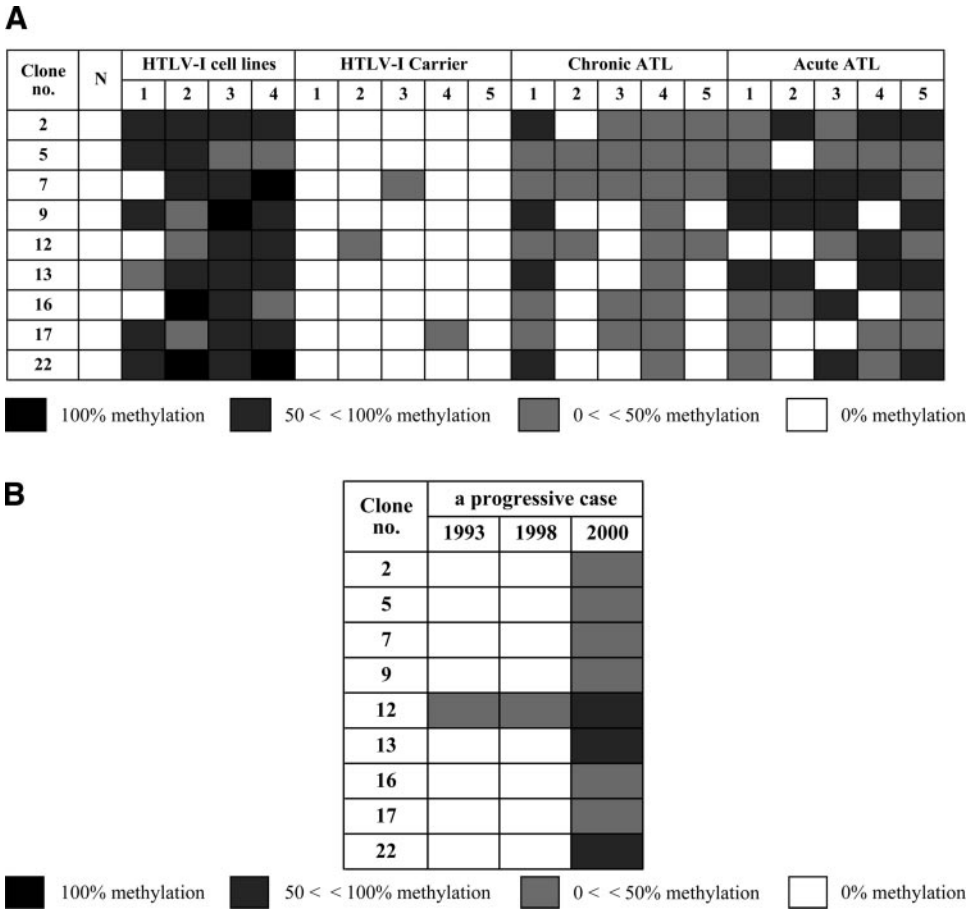

Fig. 1. Frequencies of CpG methylation of the isolated DNA regions in ATL cell lines and clinical samples. The frequencies of CpG methylation in 9 of 53 isolated regions were determined using the Combined Bisulfite Restriction Analysis method. *A*, methylation status in normal PBMCs (N), four ATL cell lines (*1*, MT-1; *2*, ATL-48T; *3*, ATL-43T; *4*, TL-Om1), and PBMCs from five asymptomatic HTLV-I carriers, five chronic ATL, and five acute ATL patients. Densities of methylation are represented by *tones of squares* as presented. *B*, serial changes of methylation status in these regions in a case with progression from carrier state to acute ATL.

treatment but not by TSA alone, suggesting that DNA methylation of *KLF4* gene is associated with its silencing in ATL cells. On the other hand, the transcript of *EGR3* gene was detected more clearly when ATL cells were treated with TSA alone or their combination than with 5-aza-dC alone, indicating that the *EGR3* gene was silenced by histone deacetylation rather than by DNA methylation. However, because demethylation by 5-aza-dC partially recovered *EGR3* gene transcription, we consider that DNA methylation is associated in part with suppressed expression of *EGR3* gene. In addition, the transcriptions of other group I genes, such as *CSPG2*, *MAFB*, and *ADRB2*, were also recovered by 5-aza-dC treatment. Because the transcription of *ADAMTS2* and *PTGDR* could not be recovered by either 5-aza-dC or TSA, the silencing of these genes might be because of other mechanism(s).

Enforced Expression of *KLF4* or *EGR3* Gene in ATL Cells. To investigate the function of *KLF4* and *EGR3* genes in ATL cells, adenovirus vectors expressing *KLF4* (KLF4-AD) or *EGR3* (EGR3-AD), were transfected into ATL-43T, in which the transcription of both genes were completely suppressed. Transfection of *KLF4*-expressing adenovirus vector induced the transcription (Fig. 4*A*) and resulted in accumulation of apoptotic cells as demonstrated by Annexin V-PI staining (Fig. 4*B*). The apoptosis was also confirmed by TUNEL assay (data not shown). The number of apoptotic cells reached maximum 48 hours later (30.1%, Fig. 4*C*). This percentage was similar to that of X-gal-stained cells (49.0%) when lacZ-AD was transfected into ATL-43T. Taken together, these results suggest that *KLF4* expression induced apoptosis in most transduced cells.

Because the *EGR3* gene is reported to be critical for *Fas ligand* (*FasL*) gene transcription (38), we studied whether enforced expression of *EGR3* could induce apoptosis of ATL cells. After transfection, both *EGR3* and *FasL* were transcribed 48 hours later (Fig. 5*A*), which coincided with increased apoptotic cells in ATL-43T infected EGR3-AD, in contrast to control (Fig. 5*B* and *C*). In addition, increased apoptotic cells were also confirmed by TUNEL assay (data not shown). Thus, enforced expression of EGR3 was considered to result in Fas-FasL-mediated apoptosis. To clarify whether this apoptosis is actually mediated by Fas signaling, we transfected vectors expressing $mCasper_L$ or E8. $mCasper_L$ is a mouse c-FLIP that inhibits the activation of procaspase 8 at the death-inducing signaling complex, whereas E8 is a viral FLIP derived from the equine herpes virus type 2. Transfection of EGR3-AD did not increase apoptosis of ATL-43T cells that expressed $mCasper_L$ and E8 (Fig. 5*A* and *C*), confirming that EGR3-induced apoptosis in ATL cell line is mediated by Fas-mediated signal.

DISCUSSION

In the present study, we identified hypermethylated DNA regions by MCA/RDA method. Consistent with the previous study (28), this method could identify hypermethylated CpG islands; 48 of 53 (91%) DNA clones identified in this study satisfied the criteria of CpG islands, and 41 of 53 (77%) DNA clones were located within 10 kb from the transcriptional start site of the nearest gene. Identified genes in the vicinity of isolated hypermethylated DNA regions could be divided into two groups; genes of group II are not expressed and not methylated in normal T lymphocytes, however, are hypermethylated in ATL cells. On the other hand, genes of group I are expressed but not methylated in normal T lymphocytes whereas their expression is suppressed in ATL cells in association with DNA methylation. It is possible that the mechanism of *de novo* methylation is dysregulated,

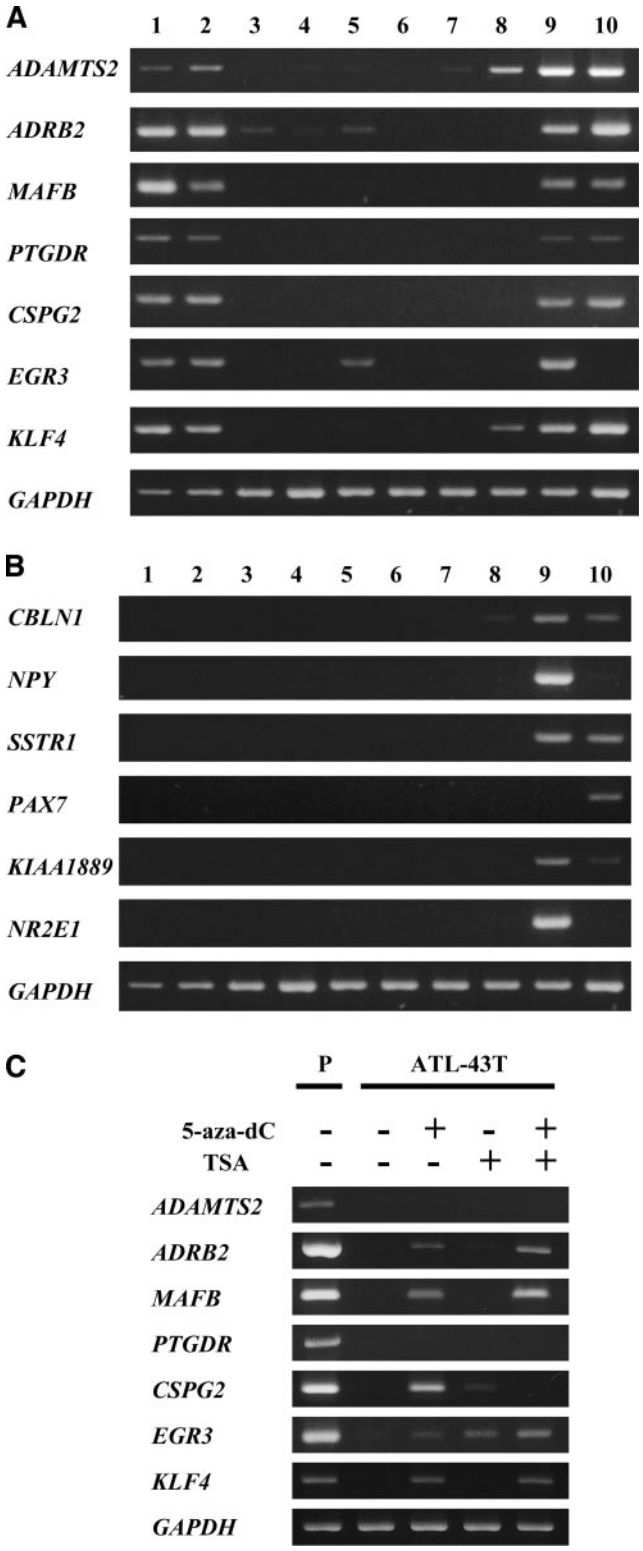

Fig. 2. Expression of genes in the vicinity of hypermethylated regions isolated by MCA/RDA. Expression of the genes near the isolated regions was studied by RT-PCR. Transcripts of the *glyceraldehyde-3-phosphate dehydrogenase* (*GAPDH*) gene were used as a control. *Lane 1*, normal resting PBMC; *Lane 2*, normal activated T cell; *Lane 3*, ED; *Lane 4*, ATL-43T; *Lane 5*, ATL-48T; *Lane 6*, ATL-55T; *Lane 7*, MT-1; *Lane 8*, MT-2; *Lane 9*, normal whole brain; *Lane 10*, normal skeletal muscle. *A*, group I, genes expressed in normal T cells but suppressed in HTLV-I-transformed and ATL cell lines. *B*, group II, genes not expressed in normal T cells and HTLV-I-associated cell lines. *C*, recovered expression of the group I genes after demethylation, ATL-43T was treated with 5-aza-dC only, TSA only, or both. Using cDNAs obtained from the treated and untreated cells, expressions of *KLF4* and *EGR3* were analyzed by RT-PCR. Phytohemagglutinin blast (P) was used as a positive control. RT-PCR of *GAPDH* was also performed to provide a control for initial RNA amounts.

resulting in aberrant methylation of genes despite their transcription as observed in group II genes. In this regard, Toyota *et al.* (28) isolated 33 hypermethylated DNA sequences in a colon cancer cell line using the MCA/RDA method and named these clones MINT1–33. Among DNA regions identified in this study, four clones were identical to MINT clones (Table 1, clone 2, clone 15, clone 30 and clone 48). These findings indicate that such DNA regions in the genome are prone to be methylated in cancer cells, which is consistent with an earlier report (22), although the factors that determine such susceptibility to methylation remain unresolved. In addition to such DNA methylation observed among different types of cancer cells, there are hypermethylated genes specifically observed in ATL cells. Analysis of DNA methylation of such genes in non-ATL T-cell lines showed that they were also methylated (data not shown), suggesting that DNA methylation of such genes is T-cell specific.

In addition to hypermethylation, we also reported hypomethylated genes in ATL cells, which included *MEL1S*, *CACNA1H*, and *Nogo receptor* genes as identified by the MCA/RDA method (30). Among them, the aberrant expression of *MEL1S* was frequently observed in ATL cells and has been shown to confer resistance against transforming growth factor-β. Thus, the MCA/RDA method indicates the involvement of both hyper- and hypomethylation in leukemogenesis of ATL although in a different manner.

In the case of *EGR3* gene, only the coding regions were methylated with little DNA methylation of the promoter region in fresh ATL cells although its expression was suppressed. TSA has more profound effect than 5-aza-dC, suggesting that histone modification, rather than DNA methylation, in the promoter region might silence the transcription of the *EGR3* gene. However, because DNA methylation in the coding region was associated with such silencing, detection of DNA methylation in non-promoter regions is also capable of identifying such silenced genes as observed in the *EGR3* gene.

EGR3 is a transcriptional factor containing zinc finger domain as well as KLF4. It has been reported that enforced expression of *EGR3* gene resulted in expression of *FasL* in HeLa cells (38), indicating that EGR3 is a critical transcriptional factor for *FasL* transcription. In agreement with these results, we also showed that expression of *EGR3* induced *FasL* transcription, resulting in apoptosis of ATL cells. Although ATL cells possess a phenotype of activated T cells and highly express Fas antigens on their surfaces, they do not produce FasL. On the other hand, normal T lymphocytes can express both Fas antigens and FasL after activation, and the number of activated T lymphocytes is regulated by Fas-FasL system-mediated apoptosis, which is designated as activation-induced cell death (39). Activation-induced cell death controls the number of activated T lymphocytes, consequently suppressing the immune response. Suppression of *EGR3* gene in ATL cells could account for lack of expression of FasL, which enables ATL cells to escape from activation-induced cell death. In the present study, we demonstrated that enforced expression of *EGR3* gene-induced FasL expression and apoptosis. Thus, because both KLF4 and EGR3 are accelerators of ATL cell apoptosis, *KLF4* and *EGR3* genes are considered new tumor-suppressor gene candidates in ATL.

KLF4 is a member of the Kruppel-like factor family, which is highly expressed in epithelial tissues such as the gut and skin, especially in the terminally differentiated cells (40, 41). Previous studies reported that KLF4 plays important roles in the regulation of G_1-S and G_2-M cell cycle checkpoint in colon cancer cells and that these functions are likely to be p53-dependent (42–44). According to these findings, KLF4 is thought to be associated with tumorigenicity of colon cancer cells. However, there is no report regarding the functional role of *KLF4* gene in lymphoid cells. Our study demonstrated that KLF4 expression induced apoptosis of ATL cells. Although the

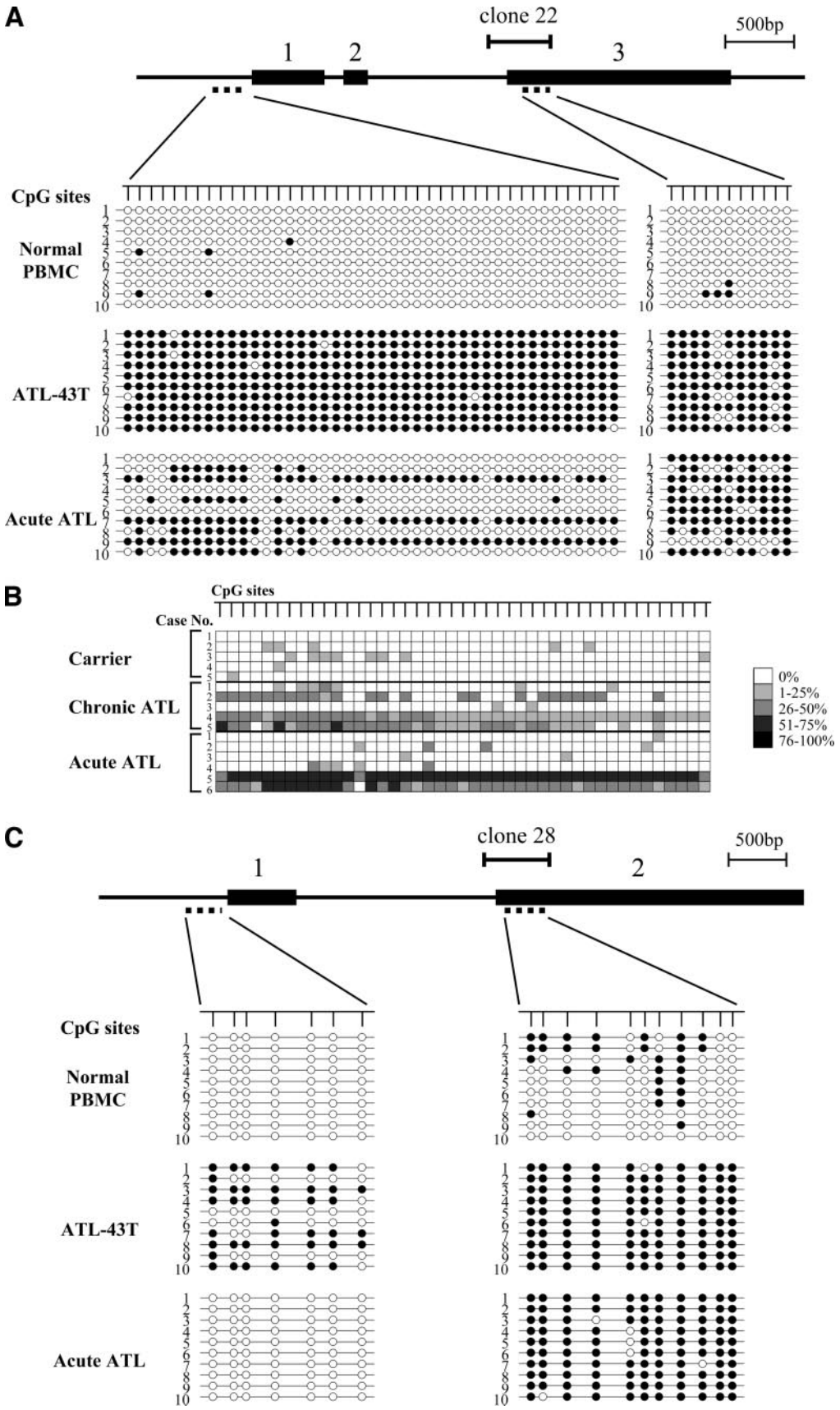

Fig. 3. Methylation status of *KLF4* and *EGR3* genes. Genomic DNAs of normal PBMC, an ATL cell line (ATL-43T), and primary cells of acute ATL were treated by sodium bisulfite and then amplified by primers specific for DNA regions in *KLF4* and *EGR3* genes identified by MCA/RDA and for their promoter regions. Then, PCR products were subcloned into plasmid DNA, and the sequences were determined in 10 clones of each (*A*, *KLF4*; *C*, *EGR3*). ○, unmethylated CpG sites; ●, methylated CpG sites. *B*, methylation status of *KLF4* promoter in primary cells with different stage of ATL; methylation level of each CpG site was calculated based on the results of bisulfite sequencing analysis and represented by *tones of squares*.

mechanism of apoptosis needs additional study, its silencing by DNA methylation facilitates the survival of ATL cells.

The present study showed that the densities of CpG methylation in identified DNA regions tend to increase with disease progression. Moreover, analysis of sequential samples from a patient who was followed from carrier state until the onset of acute ATL revealed that DNA methylation accumulated at the onset of ATL (Fig. 1*B*). These data indicate that serial analysis of the methylation status in identified hypermethylated regions might be a useful tool in the diagnosis and staging of ATL.

HTLV-I-infected clones have been shown to persist over seven years in the same HTLV-I carrier (45), suggesting that HTLV-I-infected cells survive for a long time through the action of viral proteins. On the other hand, it has been reported that aging is closely related to alterations of DNA methylation. Progressive loss of 5-methylcytosine content is observed in normal aging cells, primarily within DNA-repeated sequences. In contrast, some genes show progressive, age-related increases of DNA methylation, resulting in silencing their expressions (46). Taken together, the prolonged life span of HTLV-I-infected T cells might be a predisposing factor for aberrant DNA methylation. During the long latent period, it is possible that HTLV-I-infected cells that are adapted for survival are selected *in vivo*. In such evolution of infected cells, genetic and epigenetic changes are thought to play critical roles by suppressing the transcription of genes with tumor suppressor functions or activating the expression of genes, which exerts positive effects on survival of tumor cells.

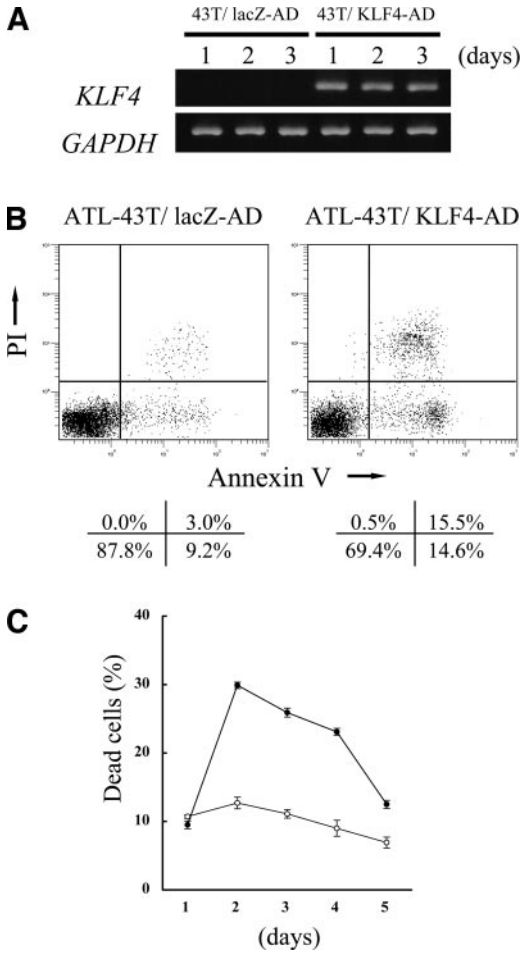

Fig. 4. Induction of apoptosis of ATL-43T by enforced expression of *KLF4*. *A*, expression of *KLF4* gene in ATL-43T transfected with lacZ-AD or KLF4-AD was studied by RT-PCR. *B*, detection of apoptotic cells in ATL-43T by double staining with Annexin V-FITC and PI at day 2 of lacZ-AD and KLF4-AD infection. The percentage of cells in each quadrant is shown at the *bottom of the panels*. *C*, serial changes in the percentages of dead cells detected by Annexin V-PI double staining. ○, ATL-43T infected with lacZ-AD; ●, ATL-43T infected with KLF4-AD. Data are mean ± SE.

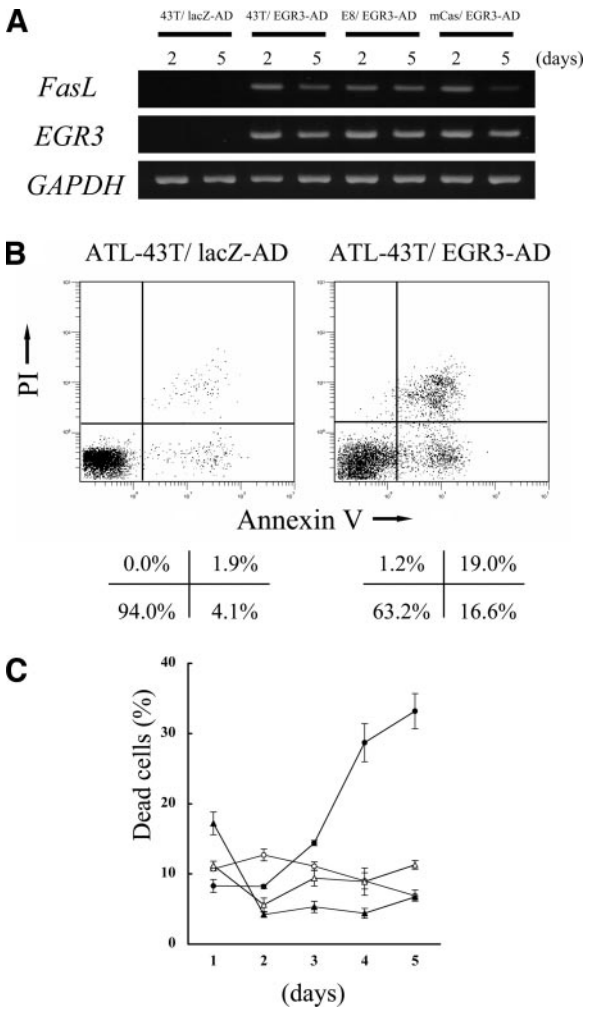

Fig. 5. Induction of *FasL* transcription and apoptosis of ATL-43T by enforced expression of *EGR3*. *A*, expressions of *EGR3* and *FasL* genes in transfected cell lines were studied by RT-PCR. *B*, detection of apoptotic cells in ATL-43T by double staining with Annexin V-FITC and PI at day 5 of lacZ-AD and EGR3-AD infection. The percentage of cells in each quadrant is shown at the *bottom of the panels*. *C*, serial changes in the percentages of dead cells detected by Annexin V-PI double staining. ○, ATL-43T infected with lacZ-AD; ●, ATL-43T infected with EGR3-AD; △, ATL-43T-mCas infected with EGR3-AD; and ▲, ATL-43T-E8 infected with EGR3-AD. Data are mean ± SE.

In conclusion, we have demonstrated in the present study that the MCA/RDA method could identify the differentially methylated DNA regions and genes according to disease progression of ATL. Such identification of aberrantly methylated genes allows for the diagnosis and staging of ATL and clarifies the molecular mechanism of leukemogenesis.

ACKNOWLEDGMENTS

We are grateful to Michiyuki Maeda for providing us valuable cell lines and to Yoshihiro Koya for valuable help. The authors also thank Dr. F. G. Issa (word-medex.com.au) for careful reading and editing of the manuscript.

REFERENCES

1. Takatsuki K, Uchiyama T, Sagawa K, Yodoi J. Adult T cell leukemia in Japan. In: Seno S, Takaku F, Irino S, editors. Topic in hematology: proceedings of the 16th international congress of Hematology, Kyoto, September 5–11, 1976. Amsterdam, Oxford: Excerpta Medica; 1977. p. 73–7.

2. Uchiyama T, Yodoi J, Sagawa K, Takatsuki K, Uchino H. Adult T-cell leukemia: clinical and hematologic features of 16 cases. Blood 1977;50:481–92.
3. Poiesz BJ, Ruscetti FW, Gazdar AF, Bunn PA, Minna JD, Gallo RC. Detection and isolation of type C retrovirus particles from fresh and cultured lymphocytes of a patient with cutaneous T-cell lymphoma. Proc Natl Acad Sci USA 1980;77:7415–9.
4. Wong-Staal F, Gallo RC. Human T-lymphotropic retroviruses. Nature (Lond) 1985; 317:395–403.
5. Arisawa K, Soda M, Endo S, et al. Evaluation of adult T-cell leukemia/lymphoma incidence and its impact on non-Hodgkin lymphoma incidence in southwestern Japan. Int J Cancer 2000;85:319–24.
6. Yoshida M. Multiple viral strategies of HTLV-1 for dysregulation of cell growth control. Annu Rev Immunol 2001;19 475–96.
7. Franchini G, Fukumoto R, Fullen JR. T-cell control by human T-cell leukemia/ lymphoma virus type 1. Int J Hematol 2003;78:280–96.
8. Jeang KT. Functional activities of the human T-cell leukemia virus type I Tax oncoprotein: cellular signaling through NF-kappa B. Cytokine Growth Factor Rev 2001;12:207–17.
9. Fujii M, Tsuchiya H, Chuhjo T, Akizawa T, Seiki M. Interaction of HTLV-1 Tax1 with p67SRF causes the aberrant induction of cellular immediate early genes through CArG boxes. Genes Dev 1992;6:2066–76.
10. Kwok RP, Laurance ME, Lundblad JR, et al. Control of cAMP-regulated enhancers by the viral transactivator Tax through CREB and the co-activator CBP. Nature (Lond) 1996;380:642–6.
11. Jeang KT, Widen SG, Semmes OJ 4th, Wilson SH. HTLV-I trans-activator protein, tax, is a trans-repressor of the human beta-polymerase gene. Science (Wash D C) 1990;247:1082–4.
12. Suzuki T, Uchida-Toita M, Yoshida M. Tax protein of HTLV-1 inhibits CBP/p300-mediated transcription by interfering with recruitment of CBP/p300 onto DNA element of E-box or p53 binding site. Oncogene 1999;18:4137–43.
13. Jin DY, Spencer F, Jeang KT. Human T cell leukemia virus type 1 oncoprotein Tax targets the human mitotic checkpoint protein MAD1. Cell 1998;93:81–91.
14. Takeda S, Maeda M, Morikawa S, et al. Genetic and epigenetic inactivation of tax gene in adult T-cell leukemia cells. Int J Cancer 2004;109:559–67.
15. Tamiya S, Matsuoka M, Etoh K, et al. Two types of defective human T-lymphotropic virus type I provirus in adult T-cell leukemia. Blood 1996;88:3065–73.
16. Furukawa Y, Kubota R, Tara M, Izumo S, Osame M. Existence of escape mutant in HTLV-I tax during the development of adult T-cell leukemia. Blood 2001;97:987–93.
17. Koiwa T, Hamano-Usami A, Ishida T, et al. 5′-long terminal repeat-selective CpG methylation of latent human T-cell leukemia virus type 1 provirus in vitro and in vivo. J Virol 2002;76:9389–97.
18. Bangham CR. Human T-lymphotropic virus type 1 (HTLV-1): persistence and immune control. Int J Hematol 2003;78:297–303.
19. Sakashita A, Hattori T, Miller CW, et al. Mutations of the p53 gene in adult T-cell leukemia. Blood 1992;79:477–80.
20. Hatta Y, Hirama T, Miller CW, Yamada Y, Tomonaga M, Koeffler HP. Homozygous deletions of the p15 (MTS2) and p16 (CDKN2/MTS1) genes in adult T-cell leukemia. Blood 1995;85:2699–704.
21. Nosaka K, Maeda M, Tamiya S, Sakai T, Mitsuya H, Matsuoka M. Increasing methylation of the CDKN2A gene is associated with the progression of adult T-cell leukemia. Cancer Res 2000;60:1043–8.
22. Costello JF, Fruhwald MC, Smiraglia DJ, et al. Aberrant CpG-island methylation has non-random and tumour-type-specific patterns. Nat Genet 2000;24:132–8.
23. Esteller M, Corn PG, Baylin SB, Herman JG. A gene hypermethylation profile of human cancer. Cancer Res 2001;61:3225–9.
24. Hayashizaki Y, Hirotsune S, Okazaki Y, et al. Restriction landmark genomic scanning method and its various applications. Electrophoresis 1993;14:251–8.
25. Gonzalgo ML, Liang G, Spruck CH, 3rd, Zingg JM, Rideout WM, 3rd, Jones PA. Identification and characterization of differentially methylated regions of genomic DNA by methylation-sensitive arbitrarily primed PCR. Cancer Res 1997;57:594–9.
26. Ushijima T, Morimura K, Hosoya Y, et al. Establishment of methylation-sensitive-representational difference analysis and isolation of hypo- and hypermethylated genomic fragments in mouse liver tumors. Proc Natl Acad Sci USA 1997;94:2284–9.
27. Huang TH, Laux DE, Hamlin BC, Tran P, Tran H, Lubahn DB. Identification of DNA methylation markers for human breast carcinomas using the methylation-sensitive restriction fingerprinting technique. Cancer Res 1997;57:1030–4.
28. Toyota M, Ho C, Ahuja N, et al. Identification of differentially methylated sequences in colorectal cancer by methylated CpG island amplification. Cancer Res 1999;59: 2307–12.
29. Ballestar E, Paz MF, Valle L, et al. Methyl-CpG binding proteins identify novel sites of epigenetic inactivation in human cancer. EMBO J 2003;22:6335–45.
30. Yoshida M, Nosaka K, Yasunaga J, Nishikata I, Morishita K, Matsuoka M. Aberrant expression of the MEL1S gene identified in association with hypomethylation in adult T-cell leukemia cells. Blood 2004;103:2753–60.
31. OhYama T, Tsukumo S, Yajima N, Sakamaki K, Yonehara S. Reduction of thymocyte numbers in transgenic mice expressing viral FLICE-inhibitory protein in a Fas-independent manner. Microbiol Immunol 2000;44:289–97.
32. Krueger A, Schmitz I, Baumann S, Krammer PH, Kirchhoff S. Cellular FLICE-inhibitory protein splice variants inhibit different steps of caspase-8 activation at the CD95 death-inducing signaling complex. J Biol Chem 2001;276:20633–40.
33. Xiong Z, Laird PW. COBRA: a sensitive and quantitative DNA methylation assay. Nucleic Acids Res 1997;25:2532–4.
34. Clark SJ, Harrison J, Paul CL, Frommer M. High sensitivity mapping of methylated cytosines. Nucleic Acids Res 1994;22:2990–7.
35. Takai D, Jones PA. Comprehensive analysis of CpG islands in human chromosomes 21 and 22. Proc Natl Acad Sci USA 2002;99:3740–5.
36. Palmisano WA, Crume KP, Grimes MJ, et al. Aberrant promoter methylation of the transcription factor genes PAX5 alpha and beta in human cancers. Cancer Res 2003;63:4620–5.
37. Cameron EE, Bachman KE, Myohanen S, Herman JG, Baylin SB. Synergy of demethylation and histone deacetylase inhibition in the re-expression of genes silenced in cancer. Nat Genet 1999;21:103–7.
38. Mittelstadt PR, Ashwell JD. Cyclosporin A-sensitive transcription factor Egr-3 regulates Fas ligand expression. Mol Cell Biol 1998;18:3744–51.
39. Krammer PH. CD95's deadly mission in the immune system. Nature (Lond) 2000; 407:789–95.
40. Shields JM, Christy RJ, Yang VW. Identification and characterization of a gene encoding a gut-enriched Kruppel-like factor expressed during growth arrest. J Biol Chem 1996;271:20009–17.
41. Segre JA, Bauer C, Fuchs E. Klf4 is a transcription factor required for establishing the barrier function of the skin. Nat Genet 1999;22:356–60.
42. Zhang W, Geiman DE, Shields JM, et al. The gut-enriched Kruppel-like factor (Kruppel-like factor 4) mediates the transactivating effect of p53 on the p21WAF1/ Cip1 promoter. J Biol Chem 2000;275:18391–8.
43. Yoon HS, Chen X, Yang VW. Kruppel-like factor 4 mediates p53-dependent G1/S cell cycle arrest in response to DNA damage. J Biol Chem 2003;278:2101–5.
44. Yoon HS, Yang VW. Requirement of Kruppel-like factor 4 in preventing entry into mitosis following DNA damage. J Biol Chem 2004;279:5035–41.
45. Etoh K, Tamiya S, Yamaguchi K, et al. Persistent clonal proliferation of human T-lymphotropic virus type I-infected cells in vivo. Cancer Res 1997;57:4862–7.
46. Issa JP. Age-related epigenetic changes and the immune system. Clin Immunol 2003;109:103–8.